Proceedings of the ASME 2011 International Mechanical Engineering Congress & Exposition
IMECE2011
November 11-17, 2011, Denver, Colorado, USA

IMECE2011-62016

MICRO-MACRO CHARACTERIZATION OF EFFECTIVE PROPERTIES FOR FIBROUS COMPOSITES WITH PARALLELOGRAM CELLS AND IMPERFECT CONTACT CONDITION

Reinaldo Rodriguez-Ramos
Facultad de Matemática y Computación, Universidad de La Habana, Habana, Cuba

Juan Carlos López-Realpozo
Facultad de Matemática y Computación, Universidad de La Habana, Habana, Cuba

Raúl Guinovart-Díaz
Facultad de Matemática y Computación, Universidad de La Habana, Habana, Cuba

Julián Bravo-Castillero
Facultad de Matemática y Computación, Universidad de La Habana, Habana, Cuba

J. A. Otero
Instituto de Cibernética, Matemática y Física. ICIMAF. La Habana, Cuba

F.J. Sabina
Instituto de Investigaciones en Matemáticas Aplicadas y en Sistemas, UNAM, DF, México

ABSTRACT

In this work, two-phase parallel fiber-reinforced periodic piezoelectric composites are considered wherein the constituents exhibit transverse isotropy and the cells have different configurations. Two types of imperfect contact at the interface of the composites are studied: a) imperfect contact via spring model, b) three phase model. Simple closed-form formulae are obtained for the effective properties of the composites with both types of contact and different parallelogram cells by means of the asymptotic homogenization method (AHM). Some numerical examples and comparisons with other theoretical results illustrate that the model is efficient for the analysis of composites with presence of parallelogram cells and imperfect contacts.

INTRODUCTION

The study of contact phenomena and the modelling of interfaces between two solids gain special importance in the effective property determination of composite media. This work is motivated by the interest to study the influence of imperfect contact over the effective piezoelectric response of oblique fibrous composites. Composites with rhombus periodic cell are important since they could describe monoclinic behavior of certain physical and biological structures. This is an extension of previous results [1,2] where perfect contact for piezoelectric composites were considered. On the other hand, in this contribution the authors extend former researches [3-5] to oblique distribution of the periodic cells under imperfect bonding contact. Two approaches (spring and three phase models) are used for the calculation of the piezoelectric effective coefficients of angular fibrous composites with anisotropic elastic constituents with no well bonded contact. This contribution is an extension of previous works [6,7] using the AHM. The results in this paper are mainly focused on the impact of the fibers cross angles and the mechanical imperfection of the interface on the stiffness properties of the chosen composites.

BASIC EQUATIONS. HETEROGENEOUS PROBLEM

Consider piezoelectric materials that respond linearly to changes in the mechanic and electric fields. A two-phase uniaxial reinforced material is considered here in which fibers and matrix have homogeneous and transversely isotropic properties; the axis of transverse symmetry coincides with the fiber direction, which is taken as the Ox_3 axis. The fiber cross-section is circular. Moreover, the fibers are periodically distributed without overlapping in directions parallel to the Ow_1- and Ow_2-axis, where $w_1 \neq 0$ and $w_2 \neq 0$ $(w_2 \neq \lambda w_1,\ \lambda \in \mathbb{R})$ are two complex numbers which define the parallelogram periodic cell of the two-phase composite. Therefore the composite Ω consists of a parallelogram array of identical circular cylinders embedded in a homogeneous medium (Fig.1). The cylinders are infinitely long. Using the conventional indicial notation in which repeated subscripts are summed over the range of $i, j, k, l = 1, 2, 3$, the constitutive equations are

$$\sigma_{ij} = C_{ijkl}\varepsilon_{kl} - e_{kij}E_k, \quad D_i = e_{ikl}\varepsilon_{kl} + \kappa_{ik}E_k, \quad (1)$$

where $\sigma_{ij}, \varepsilon_{ij}, E_i,$ and D_i are the stress tensor, strain tensor, electric field vector, and the electric displacement vector, respectively. The quantities $C_{ijkl}, e_{kij}, \kappa_{ik}$ are components of the elastic stiffness tensor, the piezoelectric tensor, and the

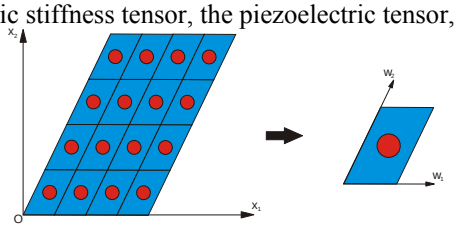

Fig. 1. The heterogeneous medium and extracted the parallelogram periodic cell.

permittivity tensor, respectively. The divergence equations, which are the elastic equilibrium as the body forces are absent, and Gauss' law, are, respectively,

$$\sigma_{ij,j} = 0, \ D_{i,i} = 0, \ \text{in } \Omega \ (2)$$

where the subscript comma denotes partial differentiation. The gradient equations, which are the strain-displacement equations and electric field-potential, are, respectively,

$$\varepsilon_{kl} = \frac{1}{2}\left(\frac{\partial u_k}{\partial x_l} + \frac{\partial u_l}{\partial x_k}\right), \ E_i = -\phi_{,i}, \ (3)$$

where u_i and ϕ are the mechanical displacement and electric potential, respectively.

Substituting (1) and (3) into (2) we obtain a coupled system of partial differential equations with coefficients rapidly oscillating

$$\left(C_{ijkl}(\mathbf{y})u^{\varepsilon}_{k,l} + e_{kij}(\mathbf{y})\phi^{\varepsilon}_{,k}\right)_{,j} = 0, \ \left(e_{ikl}(\mathbf{y})u^{\varepsilon}_{k,l} - \kappa_{ik}(\mathbf{y})\phi^{\varepsilon}_{,k}\right)_{,i} = 0 \ \text{in } \Omega. \ (4)$$

Equation (4) represents a system of equations for finding u_i and ϕ. For a complete solution, it is necessary to assign suitable boundary conditions, for instance

$$u^{\varepsilon}_i = 0; \quad \sigma^{\varepsilon}_{ij} n_j = S^0_i; \quad \phi^{\varepsilon} = \phi_0; \quad D^{\varepsilon}_i n_i = 0, \quad \text{on } \partial\Omega, \ (5)$$

where u^0_i, S^0_i and ϕ_0 are the prescribed displacement, force and electric potential on the boundary of the composite.

In order to model various possible damages occurring on the fiber-matrix interface composite two formulations of imperfect bonded are considered: a) imperfect contact via spring model, b) three phase model. The consequence of both derivations and their numerical results are studied as follows.

a) CELL PROBLEMS FOR SPRING IMPERFECT CONTACT

The inclusion problems associated with piezocomposite materials, which have been presented in the literature, are mainly concerned with perfect interface condition; see for example, [8-10]. In the case of perfect bonding, the continuities of displacement, traction, electric potential, and normal electric displacement are concerned. Often, the above electro-mechanical interface conditions are not realistic assumptions in modeling the actual physical problems. In this section it is intended to analyze the behavior of a piezocomposite under imperfect contact. The mechanical behavior of imperfect interface is modeled via a layer of mechanical springs of zero thickness. The spring constants are the measures for the magnitude of the associated continuities. The vanishing value of: K_t, K_s and K_n corresponds to pure debonding (normal perfect debonding), in-plane pure sliding, and out-of-plane pure sliding, respectively. The status of the mechanical bonding is completely determined by appropriate values of these constants. For large enough values of the constants, the perfect bonding interface is achieved.

Using the vector notation and defining the spring stiffness matrix, the mechanic displacement and the traction vectors in the following manner:

$$\mathbf{u} = \begin{pmatrix} u_t \\ u_s \\ u_n \end{pmatrix}, \ \mathbf{T} = \begin{pmatrix} T_t \\ T_s \\ T_n \end{pmatrix}, \ \mathbf{K} = \begin{pmatrix} \widetilde{K}_t & 0 & 0 \\ 0 & \widetilde{K}_s & 0 \\ 0 & 0 & \widetilde{K}_n \end{pmatrix}, \ (6)$$

the mechanical imperfect condition [11,12] in general may be expressed as

$$\mathbf{T}^{(1)} + \mathbf{T}^{(2)} = 0, \ \mathbf{T}^{(\gamma)} = (-1)^{\gamma+1}\mathbf{K}\|\mathbf{u}\|, \ \|\phi\| = 0, \ \|\mathbf{D}\|\mathbf{n} = 0 \ \text{on } \Gamma. \ (7)$$

In these relations $\|\bullet\|$ indicates the jump in the quantity at the common interface between the fiber and the matrix denoted by Γ; $\mathbf{n}$ is the outward unit normal on Γ; u_t, u_s, u_n are the tangential and normal components of the mechanic displacement vector; T_t, T_s, T_n are the tangential and normal components of the traction vector $\mathbf{T}$ ($T_i = \sigma_{ij} n_j$). The superscripts (γ), $\gamma = 1,2$ denote the matrix and fiber respectively.

Two-phase composite is considered which comprises a matrix with homogeneous properties given by the following moduli tensors: elastic $C^{(1)}_{ijkl}$, piezoelectric $e^{(1)}_{ijk}$ and dielectric permittivity $\kappa^{(1)}_{ij}$, in which are embedded parallel circular cylindrical fibers with corresponding homogeneous properties $C^{(2)}_{ijkl}$, $e^{(2)}_{ijk}$ and $\kappa^{(2)}_{ij}$. The overall properties of the above periodic medium are sought by means of the AHM [1,2]. Then, it follows that in terms of the fast variable $\mathbf{y} = \mathbf{x}/\varepsilon$, the appropriate periodic unit cell Y is taken as a regular parallelogram in the y_1y_2-plane so that $Y = Y_1 \cup Y_2$ with $Y_1 \cap Y_2 = \emptyset$, where the domain Y_1 is occupied by the matrix and its complement Y_2, a circle of radius R, is filled up with the fiber (Fig. 2). Beside the use of subscript, matrix and fiber associated quantities are also referred below by means of superscripts in brackets (1) and (2), respectively.

Under above considerations the non-ideal contact condition (7) is studied, i.e. $\widetilde{K}_n \to \infty$ and it is equivalent to $\|u_n\| = 0$. Thus the expression (7) can be re-written in the following indicial form

$$\mathbf{T}^{(1)} + \mathbf{T}^{(2)} = 0, \ \|u_n\| = 0, \ T^{(\gamma)}_t = (-1)^{\gamma+1}\widetilde{K}_t\|u_t\|, \ \text{on } \Gamma \ (8)$$
$$T^{(\gamma)}_s = (-1)^{\gamma+1}\widetilde{K}_s\|u_s\|, \ \|\phi\| = 0, \ \|D_i\|n_i = 0,$$

By means of the AHM it is possible to obtain an asymptotic solution of the boundary-value problem (4)-(5) as $\varepsilon \to 0$. The solution of (4), (5) and (8) is sought in the form

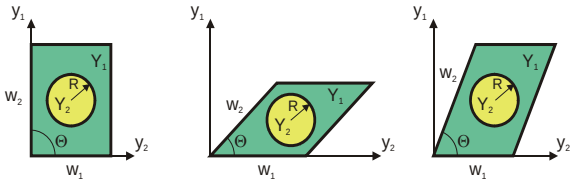

Fig. 2. Different unit cells - rectangle, rhombic and parallelogram.

of a series in powers of ε with coefficients depending on both the variables $\mathbf{x}$ and $\mathbf{y}$ treated as independent; they are referred as the slow or macroscopic and fast or microscopic variables, respectively. Here, the solution is explicitly posed as

$$\mathbf{u}^{\varepsilon}(\mathbf{x}) = \mathbf{u}^{(0)}(\mathbf{x},\mathbf{y}) + \varepsilon\mathbf{u}^{(1)}(\mathbf{x},\mathbf{y}) + \cdots,$$
$$\phi^{\varepsilon}(\mathbf{x}) = \phi^{(0)}(\mathbf{x},\mathbf{y}) + \varepsilon\phi^{(1)}(\mathbf{x},\mathbf{y}) + \cdots. \quad (9)$$

The substitution of (9) into the equations (4) and (5) and the comparison of similar powers of ε leads to the boundary value problems that are satisfied by $u_i^{(0)}, u_i^{(1)}, \phi^{(0)}$ and $\phi^{(1)}$. The relation $\mathbf{y} = \mathbf{x}/\varepsilon$, must be considered when derivatives are computed so that the chain rule is applied. It is found, to order ε^{-2}, that the functions $u_i^{(0)}$ and $\phi^{(0)}$ do not depend on $\mathbf{y}$. To the next order of ε^{-1}, due to the linearity of this problem and the assumed regularity of both the inclusions shapes and the smoothness of the coefficients, a product solution type is found for $\mathbf{u}^{(1)}$ and $\phi^{(1)}$ as follows:

$$u^{(1)}(\mathbf{x},\mathbf{y}) = {}_{pq}M(\mathbf{y})\frac{\partial u_p^{(0)}}{\partial x_q}(\mathbf{x}) + {}_{p}P(\mathbf{y})\frac{\partial \phi^{(0)}}{\partial x_q}(\mathbf{x}),$$
$$\phi^{(1)}(\mathbf{x},\mathbf{y}) = {}_{pq}N(\mathbf{y})\frac{\partial u_p^{(0)}}{\partial x_q}(\mathbf{x}) + {}_{p}Q(\mathbf{y})\frac{\partial \phi^{(0)}}{\partial x_q}(\mathbf{x}), \quad (10)$$

where the sets of $pq-$functions, ${}_{pq}M(\mathbf{y})$ and ${}_{pq}N(\mathbf{y})$, and $p-$functions, ${}_{p}P(\mathbf{y})$ and ${}_{p}Q(\mathbf{y})$, depend only on $\mathbf{y}$. They are the unique periodic solution of the so-called ${}_{pq}-$local and ${}_{p}-$local problems, denoted by ${}_{pq}L$ and ${}_{p}I$, respectively, over the periodic unit cell Y, defined below.

The ${}_{pq}L$ problem seeks displacements ${}_{pq}M^{(\gamma)}(\mathbf{y})$ and potentials ${}_{pq}N^{(\gamma)}(\mathbf{y})$, in Y_γ, $\gamma = 1,2$, which are periodic functions of periods $w_1 = 1, w_2 = be^{i\Theta}$, $b > 0$ is the modulus of this complex number and are the solution of

$$\left.\begin{array}{l} {}_{pq}\sigma_{i\delta,\delta}^{(\gamma)} = 0 \ \text{ in } Y_\gamma, \\ {}_{pq}D_{\delta,\delta}^{(\gamma)} = 0 \ \text{ in } Y_\gamma, \\ {}_{pq}\mathbf{T}^{(1)} + {}_{pq}\mathbf{T}^{(2)} = 0, \quad \left\| {}_{pq}M^{n} \right\| = 0, \left\| {}_{pq}N \right\| = 0, \\ {}_{pq}T_t^{(\gamma)} = (-1)^{\gamma+1}\widetilde{K}_t \left\| {}_{pq}M^{t} \right\|, \quad {}_{pq}T_s^{(\gamma)} = (-1)^{\gamma+1}\widetilde{K}_s \left\| {}_{pq}M^{s} \right\|, \\ \left\| {}_{pq}D_\delta \right\| n_\delta = -\left\| e_{\delta pq}^{(\gamma)} \right\| n_\delta, \end{array}\right\} \text{ on } \Gamma,$$
$$\left\langle {}_{pq}M_i \right\rangle = \left\langle {}_{pq}N \right\rangle = 0, \quad (11)$$

where

$$ {}_{pq}\sigma_{i\delta}^{(\gamma)} = C_{i\delta k\lambda}^{(\gamma)}\ {}_{pq}M_{k,\lambda}^{(\gamma)} + e_{\lambda i\delta}^{(\gamma)}\ {}_{pq}N_{,\lambda}^{(\gamma)},$$
$$ {}_{pq}D_{\delta}^{(\gamma)} = e_{\delta k\lambda}^{(\gamma)}\ {}_{pq}M_{k,\lambda}^{(\gamma)} - \kappa_{\delta\lambda}^{(\gamma)}\ {}_{pq}N_{,\lambda}^{(\gamma)}, \quad (12)$$

the comma notation denotes a partial derivative relative to the y_δ component, i.e., $U_{,\delta} \equiv \partial U/\partial y_\delta$; the summation convention is also understood for Greek indices, which run from 1 to 2; no summation is carried out over upper case indices, whether Latin on Greek. The functions ${}_{pq}M^{t}$, ${}_{pq}M^{s}$, ${}_{pq}M^{n}$ are the tangential and normal components of the vector ${}_{pq}M$ whereas ${}_{pq}T_t$, ${}_{pq}T_s$, ${}_{pq}T_n$, are the tangential and normal components of the traction vector ${}_{pq}T_i = \left({}_{pq}\sigma_{ij} + C_{ijpq}\right)n_j$ associated to the local problem ${}_{pq}L$. The angular brackets in (11), from now on, define the volume average per unit length over the unit periodic cell, that is $\langle F \rangle = \int_{|Y|} F(\mathbf{y})\,d\mathbf{y}$. The symmetry between the indices p and q shows right away that at most six problems need to be considered.

The ${}_{p}I$ problem is stated as follows: the displacements ${}_{p}P^{(\gamma)}(\mathbf{y})$ and potentials ${}_{p}Q^{(\gamma)}(\mathbf{y})$ are sought in Y_γ, $\gamma = 1,2$, which are periodic functions of periods $w_1 = 1, w_2 = be^{i\Theta}$, b is the modulus of this complex number and that satisfy the boundary-value problem

$$\left.\begin{array}{l} {}_{p}\sigma_{i\delta,\delta}^{(\gamma)} = 0 \ \text{ in } Y_\gamma, \\ {}_{p}D_{\delta,\delta}^{(\gamma)} = 0 \ \text{ in } Y_\gamma, \\ {}_{p}\mathbf{T}^{(1)} + {}_{p}\mathbf{T}^{(2)} = 0, \quad \left\| {}_{p}P^{n} \right\| = 0, \left\| {}_{p}Q \right\| = 0, \\ {}_{p}T_t^{(\gamma)} = (-1)^{\gamma+1}\widetilde{K}_t \left\| {}_{p}P^{t} \right\|, \quad {}_{p}T_s^{(\gamma)} = (-1)^{\gamma+1}\widetilde{K}_s \left\| {}_{p}P^{s} \right\|, \\ \left\| {}_{p}D_\delta \right\| n_\delta = \left\| \kappa_{\delta p}^{(\gamma)} \right\| n_\delta, \end{array}\right\} \text{ on } \Gamma,$$
$$\left\langle {}_{p}P_i \right\rangle = \left\langle {}_{p}Q \right\rangle = 0, \quad (13)$$

where the functions ${}_{p}P^{t}$, ${}_{p}P^{s}$, ${}_{p}P^{n}$ are the tangential and normal components of the vector ${}_{p}P$ whereas ${}_{p}T_t$, ${}_{p}T_s$, ${}_{p}T_n$, are the tangential and normal components of the traction vector ${}_{p}T_i = \left({}_{p}\sigma_{ij} + e_{pij}\right)n_j$ associated to the local problem ${}_{p}I$ and

$$ {}_{p}\sigma_{i\delta}^{(\gamma)} = C_{i\delta k\lambda}^{(\gamma)}\ {}_{p}P_{k,\lambda}^{(\gamma)} + e_{\lambda i\delta}^{(\gamma)}\ {}_{p}Q_{,\lambda}^{(\gamma)},$$
$$ {}_{p}D_{\delta}^{(\gamma)} = e_{\delta k\lambda}^{(\gamma)}\ {}_{p}P_{k,\lambda}^{(\gamma)} - \kappa_{\delta\lambda}^{(\gamma)}\ {}_{p}Q_{,\lambda}^{(\gamma)}. \quad (14)$$

Also the non-homogeneous ${}_{p}I$ problems will cooperate towards the homogenized moduli. The constitutive relations of the linear piezoelectric theory for a heterogeneous and periodic medium, Ω, is characterized by the $Y-$periodic functions $\mathbf{C}(\mathbf{y})$, $\mathbf{e}(\mathbf{y})$, $\boldsymbol{\kappa}(\mathbf{y})$. The original constitutive relations with rapidly oscillating material coefficients are transformed in new physical relations with constant coefficients $\mathbf{C}^*$, $\mathbf{e}^*$, $\boldsymbol{\kappa}^*$ which represent the elastic, piezoelectric and permittivity properties, respectively of an equivalent homogeneous medium and are called the effective coefficients of Ω. Therefore, the system (4) can be transformed into equivalent system with constant coefficients which represent the overall properties of the composite.

The main problem to obtain such average formulae is to find the $Y-$periodic solutions of nine ${}_{pq}L$, ${}_{p}I$ $(p,q = 1,2,3)$ local

problems on Y in terms of the fast variable $\mathbf{y}$ [1,2] based on the mathematical statement of both problems.

Once the local problems are solved, the homogenized moduli $C^*_{ijpq}, e^*_{kij}, \kappa^*_{ik}$ may be determined by using the following formulae:

$$C^*_{ijpq} = \left\langle C_{ijpq} + C_{ijkl\ pq} M_{k,l} + e_{kij\ pq} N_{,k} \right\rangle, \; e^*_{ipq} = \left\langle e_{ipq} + e_{ikl\ pq} M_{k,l} - \kappa_{ik\ pq} N_{,k} \right\rangle, \quad (15)$$
$$e^*_{pij} = \left\langle e_{pij} + C_{ijkl\ p} P_{k,l} + e_{kij\ p} Q_{,k} \right\rangle, \; \kappa^*_{ip} = \left\langle \kappa_{ip} - e_{ikl\ p} P_{k,l} + \kappa_{ik\ p} Q_{,k} \right\rangle.$$

Each local problem, (11), (13) $(p,q = 1,2,3)$ uncouples into two sets of equations. A plane-strain and an antiplane-strain systems of equations which correspond to five plane-strain local problems ${}_{pp}L$, ${}_{12}L$, ${}_{3}I$ and the fourth antiplane-strain ones ${}_{13}L$, ${}_{23}L$, ${}_{1}I$, ${}_{2}I$. The boundary-value problem set up in (11), (13) has been solved in this work using the methods of a complex variable and the properties of doubly periodic elliptic and related functions with periods w_1 and w_2 [1,2]. For simplicity, only the set of antiplane problems ${}_{13}L$, ${}_{23}L$, ${}_{1}I$, ${}_{2}I$ is explained in detail. From now on, the preindices are not used. The determination of the shear piezoelectric effective properties, denoted by $C^*_{44}, C^*_{45}, C^*_{55}$, (shear moduli), $e^*_{15}, e^*_{14}, e^*_{24}$, (shear stress piezoelectric coefficient) and $\kappa^*_{11}, \kappa^*_{12}, \kappa^*_{22}$, (transverse permittivity constant) is the main aim of this part where the constituents of each phase of the composite are of class 6mm and the short indicial notation is used. In this case the relevant constitutive relations are

$$\sigma_{23} = 2C_{44}\varepsilon_{23} - e_{15}E_2, \; \sigma_{13} = 2C_{44}\varepsilon_{13} - e_{15}E_1, \quad (16)$$
$$D_1 = 2e_{15}\varepsilon_{23} + \kappa_{11}E_1, \; D_2 = 2e_{15}\varepsilon_{13} + \kappa_{11}E_2.$$

The displacement $M \equiv {}_{13}M$ and potential $N \equiv {}_{13}N$, which appear in (15), are the unique solution of the above mentioned local problem ${}_{13}L$. In this case the equation (11) yields

$$\left.\begin{array}{l} \Delta M^{(\gamma)} = 0, \; \Delta N^{(\gamma)} = 0 \; \text{in} \; Y_\gamma \\ T^{(1)}_s + T^{(2)}_s = 0, \\ \|N\| = 0, \quad \|(e_{15}M_{,\delta} - \kappa_{11}N_{,\delta})n_\delta\| = -\|e_{15}\|n_1, \\ (C^{(\gamma)}_{44}M^{(\gamma)}_{,\delta} + e^{(\gamma)}_{15}N^{(\gamma)}_{,\delta})n_\delta + C^{(\gamma)}_{44}n_1 = (-1)^{\gamma+1}K_s C^{(1)}_{55}\|M\|R^{-1}, \\ \langle M \rangle = 0, \langle N \rangle = 0, \end{array}\right\} \text{ on } \Gamma \quad (17)$$

where Δ is the two-dimensional Laplacian.

Eqs. (15) are transformed to area integrals applying Green´s theorem. The doubly periodic boundary conditions on Y and the continuity of displacement and potential on Γ leads to

$$\begin{aligned} C^*_{55} - iC^*_{45} &= \langle C_{55} \rangle + (-1)^\gamma \frac{C^{(\gamma)}_{55}}{V}\int_\Gamma M^{(\gamma)}dy_2 + iM^{(\gamma)}dy_1 + \\ &+ (-1)^\gamma \frac{e^{(\gamma)}_{15}}{V}\int_\Gamma N^{(\gamma)}dy_2 + iN^{(\gamma)}dy_1, \\ e^*_{15} - ie^*_{25} &= \langle e_{15} \rangle + (-1)^\gamma \frac{e^{(\gamma)}_{15}}{V}\int_\Gamma M^{(\gamma)}dy_2 + iM^{(\gamma)}dy_1 + \\ &+ (-1)^\gamma \frac{\kappa^{(\gamma)}_{11}}{V}\int_\Gamma N^{(\gamma)}dy_2 + iN^{(\gamma)}dy_1. \end{aligned} \quad (18)$$

where summation convention is understood for γ, which run from 1 to 2.

Methods of potential theory are used to solve (17). Doubly periodic harmonic functions are to be found in terms of the following Laurent and Taylor expansions of harmonic functions:

$$\begin{aligned} M^{(1)}(z) &= \mathrm{Re}\left\{\frac{z}{R}a_0 + \sum_{p=1}^{\infty o}\left(\frac{R}{z}\right)^p a_p + \sum_{k=1}^{\infty o}\sum_{p=1}^{\infty o}\left(\frac{z}{R}\right)^p \eta_{kp}a_k\right\}, \\ N^{(1)}(z) &= \mathrm{Re}\left\{\frac{z}{R}b_0 + \sum_{p=1}^{\infty o}\left(\frac{R}{z}\right)^p b_p + \sum_{k=1}^{\infty o}\sum_{p=1}^{\infty o}\left(\frac{z}{R}\right)^p \eta_{kp}b_k\right\}, \text{ in } Y_1 \\ M^{(2)}(z) &= \mathrm{Re}\left\{\sum_{p=1}^{\infty o} c_p\left(\frac{z}{R}\right)^p\right\}, \; N^{(2)}(z) = \mathrm{Re}\left\{\sum_{p=1}^{\infty o} d_p\left(\frac{z}{R}\right)^p\right\}, \text{ in } Y_2 \end{aligned} \quad (19)$$

where

$$\eta_{kl} = -\frac{(k+l-1)!}{(k-1)!\,1!}R^{k+1}\sum_{m=-\infty}^{\infty}\sum_{n=-\infty}^{\infty}\frac{1}{(m\omega_1 + n\omega_2)^{k+1}}, \; m+n \neq 0, k+l > 2 \quad \text{and}$$

a_n, b_n, c_n, d_n are real undetermined coefficients; ω_1, ω_2, are the periods of the parallelogram array, respectively (see Fig. 2). The superscript "*o*" next to the summation symbol means that "p" runs only over odd integers so that each term in (19) has the same anti-symmetry property as $M^{(\gamma)}$ and $N^{(\gamma)}$, namely, $M^{(\gamma)}(-z) = -M^{(\gamma)}(z)$, $N^{(\gamma)}(-z) = -N^{(\gamma)}(z)$ (see, [1,2]).

The line integrals in (18) and the assumed expansions (19) produce a very simple result as a consequence of the orthogonality of the trigonometric functions, namely,

$$\begin{aligned} &\int_\Gamma M^{(1)}dx_2 + iM^{(1)}dx_1 = \pi R\left(\overline{a_1} + a_0 + \sum_{k=1}^{\infty o}\eta_{k1}a_k\right), \\ &\int_\Gamma N^{(1)}dx_2 + iN^{(1)}dx_1 = \pi R\left(\overline{b_1} + b_0 + \sum_{k=1}^{\infty o}\eta_{k1}b_k\right), \\ &\int_\Gamma M^{(2)}dx_2 + iM^{(2)}dx_1 = \pi R c_1, \int_\Gamma N^{(2)}dx_2 + iN^{(2)}dx_1 = \pi R d_1. \end{aligned} \quad (20)$$

Replacing (20) into Eqs. (18) and taking into consideration the imperfect contact condition (17) we obtain the final expression of the effective coefficients,

$$\begin{aligned} C^*_{55} - i\,C^*_{45} &= C^{(1)}_{55}\left(1 - 2V_2\Pi_{11}\right), \\ e^*_{15} - i\,e^*_{25} &= \sqrt{C^{(1)}_{55}\kappa^{(1)}_{11}}\left(E^{(1)} - 2V_2\Pi_{21}\right) \end{aligned} \quad (21)$$

where

$$\Pi_{11} = \overline{a_1} + E\overline{b_1}, \; \Pi_{21} = E\overline{a_1} - \overline{b_1}, \; E^{(\alpha)} = e^{(\alpha)}_{15}\Big/\sqrt{C^{(\alpha)}_{55}\kappa^{(\alpha)}_{11}},$$

the over bar denotes complex conjugate numbers, the fiber volume fraction is $V_2 = \pi R^2/V$, $V = |w_1||w_2|\sin\theta$ denotes the area of periodic cell. The unknown constants a_1, b_1 are solutions of the infinite systems related to the local problems ${}_{13}L$, in which only the residue of $M^{(\gamma)}$ and $N^{(\gamma)}$ contributes towards C^*_{55}, C^*_{45} and e^*_{15}, e^*_{25}. Thus, expressions for a_1, b_1 are now sought from the system of infinite equations

$$\mathscr{M} \times \mathscr{D} = \mathscr{U}, \quad (22)$$

where the vector $\mathscr{D}^T = (x_1, x_2, x_3, x_4)$ contains the real and imaginary parts of the unknowns $a_1 = x_1 + ix_2$, $b_1 = x_3 + ix_4$ and the vector $\mathscr{U}$ is given by $\mathscr{U}^T = R(\beta_{21}, 0, \beta_{41}, 0)$. The super

index T denotes transpose and the 4x4- order matrix $\mathcal{M}(m_{nk})$ is defined by the following matrix form,

$$\mathcal{M} = \mathcal{K} + R^2 \mathcal{G} - \mathcal{M}_1 \mathcal{P}^{-1} \mathcal{M}_2, \tag{23}$$

$$\mathcal{K} = \begin{pmatrix} \beta_{11} & 0 & \alpha_{11} & 0 \\ 0 & \beta_{11} & 0 & \alpha_{11} \\ \beta_{31} & 0 & \alpha_{31} & 0 \\ 0 & \beta_{31} & 0 & \alpha_{31} \end{pmatrix},$$

$$\mathcal{G} = \begin{pmatrix} \beta_{21}\begin{pmatrix} h_{11}+h_{12} & h_{21}-h_{22} \\ -(h_{21}+h_{22}) & h_{11}-h_{12} \end{pmatrix} & \alpha_{21}\begin{pmatrix} h_{11}+h_{12} & h_{21}-h_{22} \\ -(h_{21}+h_{22}) & h_{11}-h_{12} \end{pmatrix} \\ \beta_{41}\begin{pmatrix} h_{11}+h_{12} & h_{21}-h_{22} \\ -(h_{21}+h_{22}) & h_{11}-h_{12} \end{pmatrix} & \alpha_{41}\begin{pmatrix} h_{11}+h_{12} & h_{21}-h_{22} \\ -(h_{21}+h_{22}) & h_{11}-h_{12} \end{pmatrix} \end{pmatrix}$$

$$h_{11} = \Re e\left\{\frac{\bar{\delta}_1 \bar{w}_2 - \bar{\delta}_2 \bar{w}_1}{w_1 \bar{w}_2 - w_2 \bar{w}_1}\right\},\ h_{12} = \Re e\left\{\frac{\delta_1 \bar{w}_2 - \delta_2 \bar{w}_1}{w_1 \bar{w}_2 - w_2 \bar{w}_1}\right\},$$

$$h_{21} = \Im m\left\{\frac{\bar{\delta}_1 \bar{w}_2 - \bar{\delta}_2 \bar{w}_1}{w_1 \bar{w}_2 - w_2 \bar{w}_1}\right\},\ h_{22} = \Im m\left\{\frac{\delta_1 \bar{w}_2 - \delta_2 \bar{w}_1}{w_1 \bar{w}_2 - w_2 \bar{w}_1}\right\},$$

$\delta_\alpha = 2\zeta(w_\alpha/2)$, $\zeta(z)$ is the Zeta quasi periodic Weierstrass function defined as $\zeta(z) = \frac{1}{z} + \sum_{m,n}{}' \left(\frac{1}{z - T_{nm}} + \frac{1}{T_{nm}} + \frac{z}{T_{nm}^2}\right)$, and the prime over the summation symbol means that the pair (m, n) = (0, 0) is excluded. The Legendre's relationship links δ_1, δ_2 and the periods w_1, w_2 by the relation $\delta_1 w_2 - \delta_2 w_1 = \pi i$. The Laurent series expansion of ζ is $\zeta(z) = \frac{1}{z} - \sum_{k=2}^{\infty} c_k \frac{z^{2k-1}}{2k-1}$, where $c_1 = 0,\ c_2 = 3S_4,\ c_3 = 5S_6$ and $c_k = \frac{3}{(2k+1)(k-3)} \sum_{m=2}^{k-2} c_m c_{k-m},\ k \geq 4$. The lattice S_k is defined by $S_k = \sum_{m,n} (mw_1 + nw_2)^{-k},\ m^2 + n^2 \neq 0,\ k > 2,\ S_2 = 0$. In particular S_4 and S_6 used in the numerical implementation are reported in Table 1 of [10, 11] for parallelogram and rhombic cells respectively.

The matrices $\mathcal{M}_1, \mathcal{P}$ and $\mathcal{M}_2$ are of infinite order and for the numerical implementation it is necessary to truncate to certain order $n \in \mathbb{N}$. The matrix $\mathcal{P} = \begin{pmatrix} \mathcal{P}_{11} & \cdots & \mathcal{P}_{1n} \\ \vdots & \cdots & \vdots \\ \mathcal{P}_{n1} & \cdots & \mathcal{P}_{nn} \end{pmatrix}_{4n \times 4n}$ is composed by sub-matrices $(\mathcal{P}_{ts})_{4\times 4}$, defined by $\mathcal{P}_{ts} = \delta_{ts}\mathcal{K} + \mathcal{J}_{ts}$,

$$\mathcal{K} = \begin{pmatrix} \beta_{1\,2t+1} & 0 & \alpha_{1\,2t+1} & 0 \\ 0 & \beta_{1\,2t+1} & 0 & \alpha_{1\,2t+1} \\ \beta_{3\,2t+1} & 0 & \alpha_{32t+1} & 0 \\ 0 & \beta_{3\,2t+1} & 0 & \alpha_{3\,2t+1} \end{pmatrix},$$

$$\mathcal{J}_{ts} = \begin{pmatrix} \beta_{2\,2t+1}\begin{pmatrix} w_{12t+1\,2s+1} & -w_{22t+1\,2s+1} \\ -w_{22t+1\,2s+1} & -w_{12t+1\,2s+1} \end{pmatrix} & \alpha_{2\,2t+1}\begin{pmatrix} w_{12t+1\,2s+1} & -w_{22t+1\,2s+1} \\ -w_{22t+1\,2s+1} & -w_{12t+1\,2s+1} \end{pmatrix} \\ \beta_{4\,2t+1}\begin{pmatrix} w_{12t+1\,2s+1} & -w_{22t+1\,2s+1} \\ -w_{22t+1\,2s+1} & -w_{12t+1\,2s+1} \end{pmatrix} & \alpha_{4\,2t+1}\begin{pmatrix} w_{12t+1\,2s+1} & -w_{22t+1\,2s+1} \\ -w_{22t+1\,2s+1} & -w_{12t+1\,2s+1} \end{pmatrix} \end{pmatrix},$$

$w_{1\,kp} = \Re e(w_{kp}),\ w_{2\,kp} = \Im m(w_{kp})$, are the real and imaginary parts of the complex number $w_{kp} = \frac{(k+p-1)!}{(k-1)!(p-1)!} \frac{R^{k+p}}{\sqrt{kp}} S_{k+p}$, $k = 2t-1,\ p = 2s-1,\quad t, s = 1, 2, 3..., .$ The matrices $\mathcal{M}_1 = \begin{pmatrix} n_{41} & \cdots & n_{4n} \end{pmatrix}_{4\times 4n}$ and $\mathcal{M}_2 = \begin{pmatrix} n_{14} \\ \vdots \\ n_{n4} \end{pmatrix}_{4n\times 4}$ are composed by sub-matrices $(n_{4t})_{4\times 4}$ and $(n_{t4})_{4\times 4}$ defined by $n_{4k} = \mathcal{J}_{2t+1\,1}$, $n_{t4} = \mathcal{J}_{1\,2t+1}$ respectively. The magnitudes $\beta_{1p}, \beta_{2p}, \beta_{3p}, \beta_{4p}$, $\alpha_{1p}, \alpha_{2p}, \alpha_{3p}, \alpha_{4p}$ are given as follows,

$$\begin{aligned}
&\beta_{1p} = 1,\ \ \beta_{2p} = \frac{1 - \chi_p(1 - K_s^{-1}p)}{1 + \chi_p(1 + K_s^{-1}p)},\ \ \beta_{3p} = 1, \\
&\beta_{4p} = \frac{E^{(1)} - \sqrt{\chi_p \chi_t} E^{(2)}(1 - K_s^{-1}p)}{E^{(1)} + \sqrt{\chi_p \chi_t} E^{(2)}(1 + K_s^{-1}p)}, \\
&\alpha_{1p} = \frac{E^{(1)} + \chi_p E^{(1)} p K_s^{-1} + \sqrt{\chi_p \chi_t} E^{(2)}}{1 + \chi_p(1 + K_s^{-1}p)}, \\
&\alpha_{2p} = \frac{E^{(1)} + \chi_p E^{(1)} p K_s^{-1} - \sqrt{\chi_p \chi_t} E^{(2)}}{1 + \chi_p(1 + K_s^{-1}p)}, \\
&\alpha_{3p} = \frac{-1 + p\sqrt{\chi_p \chi_t} E^{(1)} E^{(2)} K_s^{-1} - \chi_t}{E^{(1)} + \sqrt{\chi_p \chi_t} E^{(2)}(1 + K_s^{-1}p)}, \\
&\alpha_{4p} = \frac{-1 + p\sqrt{\chi_p \chi_t} E^{(1)} E^{(2)} K_s^{-1} + \chi_t}{E^{(1)} + \sqrt{\chi_p \chi_t} E^{(2)}(1 + K_s^{-1}p)},
\end{aligned} \tag{24}$$

where $\chi_p = C_{44}^{(2)} / C_{44}^{(1)},\ \chi_t = \kappa_{11}^{(2)} / \kappa_{11}^{(1)}$.

The limit case of perfect contact condition for piezoelectric antiplane problem is derived as a particular case of (22)-(24) as $K_s \to \infty$. In this case, the parameters a_1, b_1 are the same that in ([1], see formula (3.25), page 1475). The infinite system (22)-(24) is used such that it is truncated for obtaining a $n \times n$ order system. It is interesting to note that the effective properties are monotonic function of order n of the solution of the system. The numerical results converge well to the exact solutions when an adequate order in the solution of the system is chosen as N increase. The truncation order for solving the system increases as the parameters K, χ^* and the fiber volume fraction are high. In the numerical examples the solutions are given for $N = 10$, because this order of n achieves the require accuracy for the parameters used.

The remaining antiplane problems ${}_{23}L$, ${}_{1}I$, ${}_{2}I$ can be solved in analogous form to the aforementioned problem. As a summary, all the effective coefficients derived from the antiplane set of local problems can be listed as follows,

$$\begin{aligned}
&C_{55}^* - i\,C_{45}^* = C_{55}^{(1)}(1 - 2V_2 H_{11}), \\
&C_{45}^* - i\,C_{44}^* = -C_{55}^{(1)}(i + 2V_2 H_{12}), \\
&e_{15}^* - i\,e_{25}^* = \sqrt{C_{55}^{(1)} \kappa_{11}^{(1)}}(E - 2V_2 H_{21}), \\
&e_{14}^* - i\,e_{24}^* = -\sqrt{C_{55}^{(1)} \kappa_{11}^{(1)}}(iE + 2V_2 H_{22}), \\
&\kappa_{11}^* - i\,\kappa_{12}^* = \kappa_{11}^{(1)}(1 + 2V_2 H_{31}), \\
&\kappa_{12}^* - i\,\kappa_{22}^* = -\kappa_{11}^{(1)}(i - 2V_2 H_{31})
\end{aligned} \tag{25}$$

where

$H_{1\alpha} = \overline{a}_{1(\alpha 3)} + E\overline{b}_{1(\alpha 3)}$, $H_{2\alpha} = E\overline{a}_{1(\alpha 3)} - \overline{b}_{1(\alpha 3)}$,

$H_{3\alpha} = E\overline{a}_{1(\alpha)} - \overline{b}_{1(\alpha)}$, $H_{4\alpha} = \overline{a}_{1(\alpha)} + E\overline{b}_{1(\alpha)}$, $E = e_{113}^{(1)} \Big/ \sqrt{C_{1313}^{(1)} \kappa_{11}^{(1)}}$,

the over bar denotes complex conjugate numbers and $a_{1(\alpha 3)}$, $b_{1(\alpha 3)}$, $a_{1(\alpha)}$ and $b_{1(\alpha)}$ are solution of the infinite systems related to the local problems ${}_{13}L$, ${}_{23}L$, ${}_{1}I$ and ${}_{2}I$.

THREE-PHASE MODEL

The imperfect interface condition (8) is replaced by the explicit three-phase problem of two constituents and an interphase of certain thickness (t), with two perfect interfaces conditions at Γ_1 and Γ_2 (Fig. 3). The region occupied by the matrix, the fiber and the interphase in the periodic cell are denoted by Y_1, Y_2 and Y_I respectively. The common region between the matrix Y_1 and the interphase Y_i is a circumference of radio $R + t$, denoted by Γ_1 where t is the thickness of interphase. The common region between the interphase Y_i and the fiber Y_2 is a circumference of radio R denoted by Γ_2 (see in Fig. 3 the corresponding periodic cell).

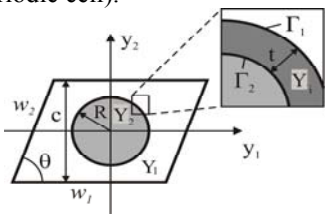

Fig. 3. Parallelogram periodic cell of composite, with a thickness interphase t of another material between the matrix and fiber.

The statement and the solution of the local problems as well as the effective coefficients for three phase models are calculated in analogous way to the spring interface model reported previously. The closed form expressions of the effective coefficients were reported in [13] and they are unknown functions of the interphase properties. Prior work has established that for mechanical imperfections, a relation between the spring and interphase parameters was found [14,15].

ANALYSIS OF RESULTS

In the present work, from the expressions (25) for rhombic periodic cells with periods $w_1 = 1, w_2 = e^{i\theta}$, $\theta = 60^o$ or $\theta = 90^o$ a composite with hexagonal or tetragonal crystal classes [16] respectively are obtained as in [1,2].

Now, the effects of the angle of inclination of the cell and the imperfection of the interface composites are illustrated. Only the consequences of the set of antiplane problems ${}_{13}L$, ${}_{23}L$, ${}_{1}I$, ${}_{2}I$ are given.

In Table 1 two phase composites Epoxy matrix/ PZT-7A fiber with rectangular periodic cell ($w_1 = 1, w_2 = bi$ see Fig. 2a) and perfect contact condition (spring model, $K_s = 10^8$) is considered. The materials parameters are $C_{44}^{(1)} = 1.8$ GPa, $\kappa_{11}^{(1)} = 0.0372$ C / Vm, and $C_{44}^{(2)} = 25.7$ GPa, $e_{15}^{(2)} = 9.35$ Cm^2, $\kappa_{11}^{(2)} = 4.065$ C / Vm. Comparison between the asymptotic homogenization method and eigenfunction expansion-variational method (EEVM) [17] are reported in order to validate the present model. The set of effective moduli $C_{44}^*, e_{24}^*, \kappa_{22}^*$ decreases as the height of the rectangle cell increases. In other words, $C_{44}^*, e_{24}^*, \kappa_{22}^*$ become stronger for small values of the height of the rectangle cell. On the other hand, $C_{55}^*, e_{15}^*, \kappa_{11}^*$ increase as the height of the rectangle cell increases as well. This trend is due to the augment of the distance between the fibers in y_2 direction in this case of composite cell.

Table 1		b=1.1		b=2	
V_2		0.1	0.3	0.1	0.3
C_{55}^* GPa	AHM	2.17	3.26	2.21	4.31
	EEVM	2.17	3.26	2.21	4.31
e_{15}^* (C/m^2)	AHM	0.00	0.01	0.00	0.03
	EEVM	0.00	0.01	0.00	0.03
κ_{11}^* (C/Vm)	AHM	0.05	0.07	0.05	0.10
	EEVM	0.05	0.07	0.05	0.10
C_{44}^* (GPa)	AHM	2.16	3.13	2.13	2.79
	EEVM	2.16	3.13	2.13	2.79
e_{24}^* (C/m^2)	AHM	0.00	0.01	0.00	0.00
	EEVM	0.00	0.01	0.00	0.00
κ_{22}^* (C/Vm)	AHM	0.05	0.07	0.04	0.06
	EEVM	0.05	0.07	0.04	0.06

Table 1. Composites with rectangular periodic cells ($w_1 = 1, w_2 = bi$ see Fig. 2a). Comparison between AHM and EEVM.

Table 2 illustrates the behavior of all effective coefficients calculated by AHM and EEVM for two-phase composites Epoxy matrix/ PZT-7A fiber with rhombic periodic cell and perfect contact condition (spring model, $K_s = 10^8$). The volume fraction of the fiber used in the computation is $V_2 = 0.6$. The numerical results derived by AHM and EEVM are the same. The influence of the arrangement of the cells in the composite can be observed. The table is grouped according to the independent components: elastic, piezoelectric, dielectric. All effective properties coincide at the angles 60^o and 90^o, i.e., $C_{44}^* = C_{55}^*$, $e_{24}^* = e_{15}^*$, $\kappa_{22}^* = \kappa_{11}^*$, $C_{45}^* = e_{14}^* = \kappa_{12}^*$. The difference between the coefficients is remarkable for the angle of the cell of 45^o. The explanation should be given due to the fact that in the short diagonal of the rhombic cell the distance between the fibers is small and this fact reinforces the properties of the composite in this direction.

In Table 3 a comparison of the effective properties between AHM and EEVM is shown for Epoxy/ PZT-7A composite with parallelogram periodic cells and perfect contact condition (spring model, $K_s = 10^8$). The global behavior of composites with

periodic cells $w_1 = 1, w_2 = 1/2 + bi$ (b=1, b=1.5) is orthorhombic of class 2mm.

$V_2 = 0.6$	45°		75°		90°	
	AHM	EEVM	AHM	EEVM	AHM	EEVM
C^*_{55} (GPa)	5.96	5.96	6.61	6.61	6.67	6.67
C^*_{54} (GPa)	-1.68	-1.69	0.32	0.32	0.00	0.00
C^*_{45} (GPa)	-1.68	-1.69	0.32	0.32	0.00	0.00
C^*_{44} (GPa)	9.33	9.33	6.44	6.44	6.67	6.67
e^*_{15} (C/m^2)	0.05	0.05	0.05	0.05	0.05	0.05
e^*_{14} (C/m^2)	-0.06	-0.06	0.01	0.01	0.00	0.00
e^*_{25} (C/m^2)	-0.06	-0.06	0.01	0.01	0.00	0.00
e^*_{24} (C/m^2)	0.16	0.16	0.05	0.05	0.05	0.05
κ^*_{11} (C/Vm)	0.14	0.14	0.16	0.16	0.16	0.16
κ^*_{12} (C/Vm)	-0.06	-0.06	0.01	0.01	0.00	0.00
κ^*_{21} (C/Vm)	-0.06	-0.06	0.01	0.01	0.00	0.00
κ^*_{22} (C/Vm)	0.25	0.25	0.15	0.15	0.16	0.16

Table 2. Effective properties by AHM and EEVM for two-phase composites with rhombic periodic cell ($w_1 = 1, w_2 = e^{i\theta}$, see Fig. 2b).

The percolation limit, that is, the volume when the fibers are in contact, changes according with the configuration of the cells. For instance, the case b=1.5 requires maximal percolation limit of $V_2 = 0.52$, whereas for the case b=1 the percolation limit is $V_2 = 0.785$. Notice that all effective properties increase as the fiber volume fraction increases as well.

In Fig. 4 the effective properties $C^*_{44}, C^*_{45}, C^*_{55}$, (shear moduli), $e^*_{15}, e^*_{14}, e^*_{24}$, (shear stress piezoelectric coefficient) and $\kappa^*_{11}, \kappa^*_{12}, \kappa^*_{22}$, (transverse permittivity constant) are shown for composites with different configuration of rhombic cells ($\theta = 45^o, \theta = 60^o, \theta = 75^o$ and $\theta = 90^o$) under imperfect bonded contact. The following values of the composites were used: $V_2 = 0.5$, $C^{(2)}_{44} / C^{(1)}_{44} = 120$, $e^{(2)}_{15} / e^{(1)}_{15} = 20$, $\kappa^{(2)}_{11} / \kappa^{(1)}_{11} = 10$.

As a particular case, we will examine elastic two-phase composites. The effect of elastic interface imperfection on shear dimensionless effective coefficients $C^*_{44} / C^{(1)}_{44}$, $C^*_{55} / C^{(1)}_{55}$ for an anisotropic composite made of T300 fibers embedded in an Epoxy matrix is shown in Figs. 5-6. The material parameters are taken from Hashin [18]. The effective properties are calculated by the two AHM imperfect contact approaches: spring model (red discontinuos line) and three-phase models (yellow circles), considering a rhombic periodic cell with $\theta = 30^0$ and three different volume fiber fraction $V_2 = 0.4$ (square), $V_2 = 0.3$ (triangle) and $V_2 = 0.2$ (star).

The comparisons illustrate that the two models are coincident, where the relationship between the non-dimensional debonding parameter K_s and the interphase property κ_1 can be introduced as $K_s = R\kappa_1 / t$ (see [15]) and it is used in the computation. The anisotropic character of this composite can be observed in Figs 5-6 where the values of the coefficient for $C^*_{44} / C^{(1)}_{44}$ reaches higher values than the one obtained for $C^*_{55} / C^{(1)}_{55}$, mainly for perfect contact $K_s \to \infty$. The more pronounced effective properties are obtained for the higher volume fraction for $K_s > 1$, the opposite situation is obtained for $K_s < 1$ because of the total disjoint between the matrix and fibers. The properties are almost independent of the volume fraction as $K_s = 1$. Another remark is related to the rapid increasing of the properties when the imperfect parameter K_s is in the neighborhood of 1. For other cases, the overall properties are constant. This situation is the same as shown Hashin [18] (in Figure 3) for isotropic composite and hexagonal symmetry ($\theta = 60^0$).

Table 3		b=1				b=1.5		
V_2		0.1	0.3	0.5	0.7	0.1	0.3	0.5
C^*_{44} (GPa)	AHM	2.16	3.14	4.69	7.63	2.15	2.94	3.96
	EEVM	2.16	3.14	4.69	7.63	2.15	2.94	3.96
C^*_{55} (GPa)	AHM	2.17	3.24	5.20	10.55	2.19	3.59	9.88
	EEVM	2.17	3.24	5.20	10.55	2.19	3.59	9.88
e^*_{15} (C/m^2)	AHM	0.00	0.01	0.03	0.16	0.00	0.01	0.26
	EEVM	0.00	0.01	0.03	0.16	0.00	0.01	0.26
e^*_{24} (C/m^2)	AHM	0.00	0.01	0.02	0.06	0.00	0.00	0.01
	EEVM	0.00	0.01	0.02	0.06	0.00	0.00	0.01
κ^*_{11} (C/Vm)	AHM	0.05	0.07	0.12	0.28	0.05	0.08	0.30
	EEVM	0.05	0.07	0.12	0.28	0.05	0.08	0.30
κ^*_{22} (C/Vm)	AHM	0.05	0.07	0.10	0.18	0.04	0.06	0.09
	EEVM	0.05	0.07	0.10	0.18	0.04	0.06	0.09

Table 3. Effective properties of composites with parallelogram cells ($w_1 = 1, w_2 = 1/2 + bi$ see Fig. 2c).

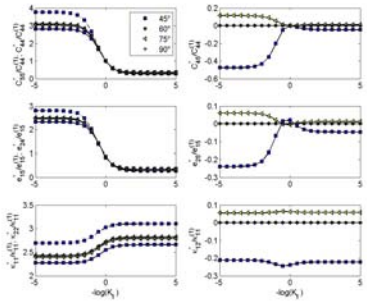

Fig. 4. Elastic, piezoelectric and dielectric effective properties for composites with different rhombic cells and imperfect bonded. The coefficients $C^*_{55} / C^{(1)}_{44}, e^*_{15} / e^{(1)}_{15}, \kappa^*_{11} / \kappa^{(1)}_{11}$ are denoted by (+-continue line) and $C^*_{44} / C^{(1)}_{44}, e^*_{24} / e^{(1)}_{15}, \kappa^*_{22} / \kappa^{(1)}_{11}$ (+-discontinue line) in each figure.

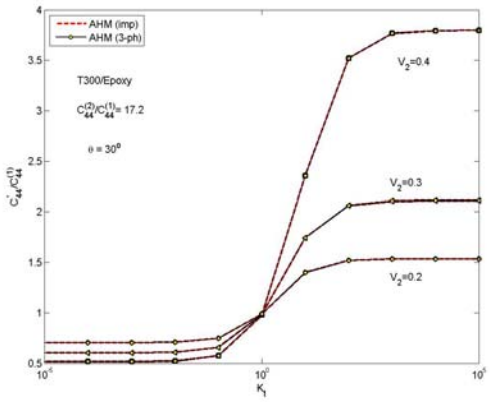

Fig. 5. Effect of elastic interface imperfection on shear dimensionless effective coefficient $C_{44}^* / C_{44}^{(1)}$ for an anisotropic composite T300 fibers and Epoxy matrix for different fiber volume fraction.

As it is well known, mechanical and thermal conductivity nature can be derived from the antiplane problem. Figs. 7-8 show the effective thermal conductivities of unidirectional fiber composites with square periodic cell with different thermal barrier giving by the parameter α. Only one effective properties is studied because the composite is isotropic and $C_{44}^* / C_{44}^{(1)} = C_{55}^* / C_{55}^{(1)}$, $C_{45}^* / C_{44}^{(1)}$. The effective thermal conductivities for different values of imperfect parameter are analogously presented to those reported in Fig. 4 by Andrianov et al. [19]. A comparison between the three-phase and the spring models for imperfect contact is shown for periodic cell with $\theta = 90^0$ and the two ratios $C_{44}^{(2)} / C_{44}^{(1)} = 666$ and $C_{44}^{(2)} / C_{44}^{(1)} = 4.4$. The non-dimensional debonding parameter α, $0 \le \alpha \le 1$ can be introduced as follows $K_s = (1-\alpha)/\alpha$, where $\alpha = 0$ denotes the perfect contact between the phases and $\alpha = 1$ represents the complete separation in the composite.

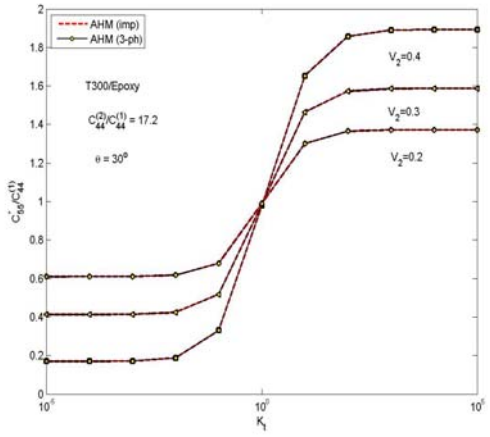

Fig. 6. Effect of elastic interface imperfection on shear dimensionless effective coefficient $C_{55}^* / C_{55}^{(1)}$, for an anisotropic composite T300 fibers and Epoxy matrix for different fiber volume fraction.

Figs. 7-8 compare the present analytical predictions for both models (spring and three phase) with the existing experimental data (the cross symbols), taking from Zou et al. [20] for perfect interface ($\alpha = 0$). Very good coincidence between these models for different values of α in the whole range of fiber volume fraction can be observed.

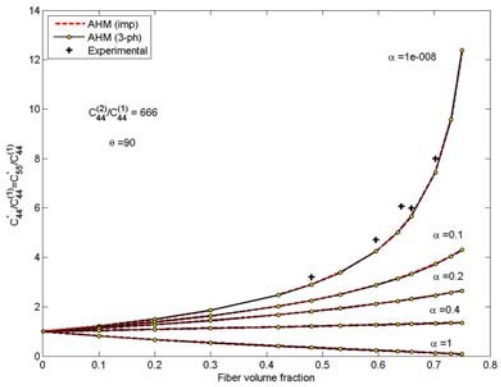

Fig. 7. Comparison between the three-phase and the spring model for different imperfect parameters α, square periodic cell and ratio $C_{44}^{(2)} / C_{44}^{(1)} = 666$ with the existing experimental data (the cross symbols), taking from Zou et al. [20], for perfect interface.

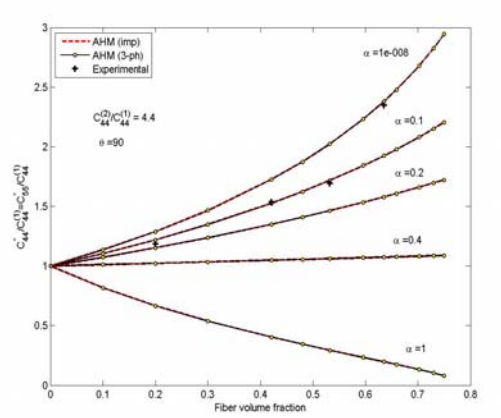

Fig. 8. Comparison between the three-phase and the spring model for different imperfect parameters α, square periodic cell and ratio $C_{44}^{(2)} / C_{44}^{(1)} = 4.4$ with the existing experimental data (the cross symbols), taking from Zou et al. [20], for perfect interface.

The effective property $C_{44}^* / C_{44}^{(1)}$ become weaker in comparison with perfect contact $\alpha = 0$, as a consequence of the imperfectly bonded matrix with fibers. It is seen from Fig. 7 that a good agreement between the present analytical models and experimental data is found, for a composite without tiny thermal barrier ($\alpha = 10^{-8}$). This situation can be considered as a perfect case. It is worthy pointing out that in Fig. 8, when a proper thermal resistance or barrier is considered ($\alpha \neq 0$), an excellent agreement between the present analytical expressions and the existing experimental data can be obtained for $\alpha = 0.1$. This means that a proper thermal barrier should be included in a theoretical model for a more accurate prediction of real thermal conductivities. Similar analysis is presented in figure (4) of Zou

et al. [20]. Notice that, Fig 8 shows more deviation than Figure 7 for the last experimental result because the experiment didn't achieve a perfect thermal barrier.

AN APPLICATION TO BIOLOGICAL STRUCTURES

Sometimes, composite materials may be regarded as an idealized model of certain biological tissue comprising tubular cells, such as skeletal muscle [21], bones, etc and the applications of the present models of composites to biological tissue is of great interest. In particular tissues that are made of growing and non-growing components. Therefore, an application of the composites to mechanical of tissue is studied in the following example.

Equations (18) have been derived under the hypothesis that material ratio $\kappa = C_{44}^{(2)}/C_{44}^{(1)}$ and the imperfection parameter K are real quantities. However, the constituents and the effective properties are, in general, complex numbers [21]. Assuming this hypothesis, the analytical expressions (18) are transformed in order to obtain the effective complex conductivity p and q of an biological specimen with interfacial impedance K where constituents and interphasial parameters are taken as complex numbers as in [21]. It is well known, that $p = q$ for transversely isotropic composites. Due to the often anisotropic character of the periodic composite with parallelogram cell we have that $p \neq q$. The effective properties can be computed by the following analytical formulae

$$p = C_{55}^{*} - iC_{45}^{*} = p_1\left(1 - 2V_2\frac{\beta_{11}(z_{22}+iz_{21})+\beta_{21}(z_{12}+iz_{11})}{|Z|}\right), \quad (26)$$

$$q = C_{44}^{*} + iC_{54}^{*} + = = -p_1 i\left(i + 2V_2\frac{\beta_{21}(z_{22}+iz_{21})-\beta_{11}(z_{12}+iz_{11})}{|Z|}\right),$$

for a two-phase fibrous composite material composed of a periodic parallelogram arrangement of identical circular cylinders embedded in a matrix with radius R and electric conductivity in each phase p_1 and p_2 respectively . The composite material represents an idealized model of a biological tissue comprising tubular cells, such as skeletal muscle. Cells are coated by plasma membranes, which are dielectric lipid bilayers. Their thickness is of the order of ten nanometers, much smaller than the spatial period l of the microstructure, which is of the order of ten micrometers. The plasma membranes can be modeled as two-dimensional interfaces between the intra- and extra-cellular phases, with conductance B and capacitance C per unit area respectively given by the electric conductivity and permittivity of the bilayer, divided by its thickness, see, [21]. Hence, the interface admittance per unit area is denoted by $\tilde{K} = B + i\omega C$, where ω is the circular frequency. This finite interface admittance causes the electric potential to jump across the interfaces, and then they are usually referred to as imperfect.

Fig. 9 shows a comparison with the results obtained by [21] (red circles, BC) for different periodic parallelogram cell, where $w_1 = 1$, $w_2 = 1/2 + bi$, with $V_2 = 0.62$ and different values of b (Fig.1b). The composite with hexagonal (black cross, $b = 0.886$) and squared (blue square, $b = 0.5$) cells are isotropic, the effective properties satisfies $p = q$. Moreover, Fig. 9 illustrates the effective properties of an orthotropic composite with rhombic periodic cell $b = 1.25$ (green triangle). Fig. 9(a) shows the real parts $(\Re(p)\ ;\Re(q))$ of effective coefficients p and q versus the dimensionless circular frequency Ω. For the composite with $b = 1.25$, the angle of periodic cell is $\theta = 68.2^{o}$ and $\Re(p) \neq \Re(q)$. Fig. 9(b)-(c) displays the imaginary parts

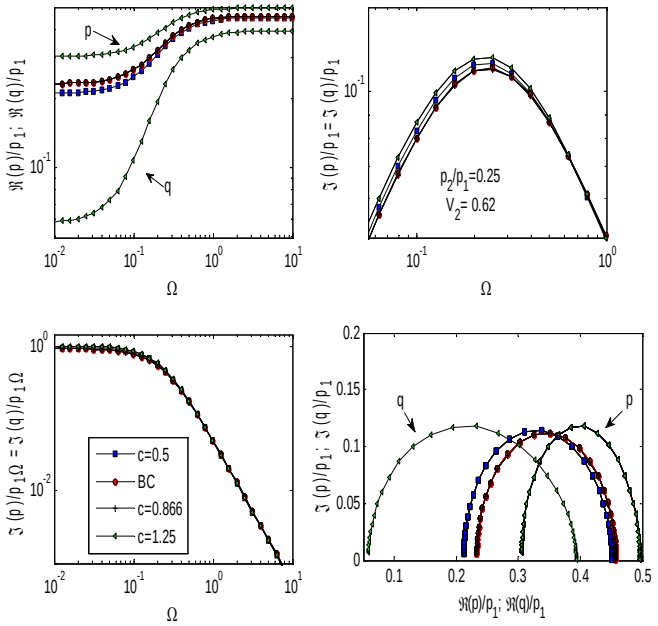

Fig. 9. Comparison with the results obtained by (22) (red circles, BC) for different periodic parallelogram cell, $w_1 = 1$, $w_2 = 1/2 + bi$, with $V_2 = 0.62$ and different values of b (Fig.1b). The composite with hexagonal (black cross, $b = 0.886$) and squared (blue square, $b = 0.5$) cells are isotropic, the effective properties satisfies $p = q$. Fig. 9(a) the real parts $(\Re(p)\ ;\Re(q))$ of effective coefficients p and q versus the dimensionless circular frequency Ω. Fig. 9(b)-(c) the imaginary parts $(\Im(p)\ ;\Im(q))$ of effective coefficients p and q versus the dimensionless circular frequency Ω. Fig. 9(d) the imaginary parts $(\Im(p)\ ;\Im(q))$ versus the real parts $(\Re(p)\ ;\Re(q))$.

$(\Im(p)\ ;\Im(q))$ of effective coefficients p and q versus the dimensionless circular frequency Ω. From Eq.(26), it is obtained that $\Im(p) = \Im(q)$ for any composite. Fig. 9(d) shows the imaginary parts $(\Im(p)\ ;\Im(q))$ versus the real parts $(\Re(p)\ ;\Re(q))$. The results obtained in Eq. (26) are qualitatively consistent for isotropic composite with the results reported by [22]. The novelty of this contribution in comparison with [22], reveals that an small change in the angle or periodicity of composite $(\theta = 68.2^{o})$, in comparison with the hexagonal case,

introduce a different global behavior in the effective complex conductance.

CONCLUSIONS

The local problems associated to an anisotropic piezoelectric composite with mechanical imperfect interface condition and rhombus cell is formulated. The mechanical imperfections such as in-plane and out-of-plane sliding and normal debonding are modeled by their corresponding mechanical springs at the interface and three phase model. The effect of the inclination of the cell leads to monoclinic anisotropic behavior in the composite.

ACKNOWLEDGMENTS

The funding of Conacyt project number 129658 is gratefully acknowledged.

REFERENCES

[1] Bravo-Castillero, J., Guinovart Díaz, R., Sabina F. J., Rodríguez Ramos, R., 2001, "Closed-form expressions for the effective coefficients of a fiber-reinforced composite with transversely isotropic constituents-II. Piezoelectric and square symmetry," Mech. Mater., 33 (4), 237-248.

[2] Sabina, F. J, Rodríguez Ramos, R., Bravo Castillero, J., Guinovart Díaz, R., 2001, "Closed-form expressions for the effective coefficients of fibre-reinforced composite with transversely isotropic constituents-II: Piezoelectric and hexagonal symmetry," J. Mech. Phys. Solids, 49, 1463-1479.

[3] Molkov, V. A., Pobedria, B. E., 1988, "Effective elastic properties of a composite with elastic contact," Izvestia Akademia Nauk SSR, Mekh. Tverdovo Tela No. 1, 111-117.

[4] Guinovart-Díaz, R., López-Realpozo, J. C., Rodríguez-Ramos, R., Bravo-Castillero, J., Ramírez, M., Camacho-Montes, H., Sabina, F. J., 2011, "Influence of parallelogram cells in the axial behaviour of fibrous composite," Int. J. Eng. Sci., 49, 75-84.

[5] Rodríguez-Ramos, R., Guinovart-Diaz, R., López, J. C., Bravo-Castillero, J., Sabina, F. J., 2010, "Influence of imperfect elastic contact condition on the antiplane effective properties of piezoelectric fibrous composites," Arch. Appl. Mech., 80, 377-388.

[6] Rodríguez-Ramos, R., Yan, P., López-Realpozo, J. C., Guinovart-Díaz, R., Bravo-Castillero, J., Sabina, F. J., Jiang, C. P., 2011, "Two analytical models for the study of periodic fibrous elastic composite with different unit cells," Comp. Struct., 93, 709-14.

[7] Guinovart-Díaz, R., López-Realpozo, J. C., Rodríguez-Ramos, R., Bravo-Castillero, J., Ramirez, M., Camacho-Montes, H., Sabina, F. J., 2010, "Influence of parallelogram cells in the axial behaviour of fibrous composite," Int. J. Eng. Sci., 49, 75-84.

[8] Pak, Y. E., 1992, "Circular inclusion problem in antiplane piezoelectricity," Int. J. Solids Struct., 29 (19), 2403-2419.

[9] Sosa, H. A., 1991, "Plane problems in piezoelectric media with defects," Int. J. Solids Struct., 28 (4), 491-505.

[10] Xiao, Z. M., Bai, J., 1999, "On piezoelectric inhomogeneity related problem-part I: a close-form solution for the stress field outside a circular piezoelectric inhomogeneity," Int. J. Eng. Sci., 37, 945-959.

[11] Hashin, Z., 1990, "Thermoelastic properties of fiber composites with imperfect interface," Mech. Mater., 8, 333-348.

[12] Shodja, H. M., Tabatabaei, S. M., Kamali, M. T., 2006, "A piezoelectric-inhomogeneity system with imperfect interface," Int. J. Eng. Sci., 44, 291-311.

[13] Guinovart-Díaz, R., Rodríguez-Ramos, R., Bravo-Castillero, J., Sabina, F. J., Camacho-Montes, H., 2008, "Electromechanical moduli of three-phase fiber composites," Mat. Lett., 62, 2385-2387.

[14] Hashin, Z., 2002, "Thin interphase/imperfect interface in elasticity with application to coated fiber composites," J. Mech. Phys. Solids, 50, 2509-2537.

[15] Lopez-Realpozo, J. C., Rodriguez-Ramos, R., Guinovart-Diaz, R., Bravo-Castillero, J., Sabina, F. J., 2011, "Transport properties in fibrous elastic rhombic composite with imperfect contact condition," Int. J. Mech. Sci. 53, 98-107, 2011.

[16] Royer D., Dieulesaint E., 2000, Elastic waves in Solids I. Berlin, Heidelberg: Springer Verlag.

[17] Yan, P., Jiang, C. P., Song, F. "An eigenfunction expansion-variational method for the anti-plane electroelastic behavior of three-phase fiber composites," Mech. Mater. (in press).

[18] Hashin Z., 1990, "Thermoelastic properties of fiber composites with imperfect interface," Mech. Mater., 8, 333-338.

[19] Andrianov, I. V., Bolshakov, V. I., Danishevs´kyy, V. V., Weichert, D., 2007, "Asymptotic simulation of imperfect bonding in periodic fibre-reinforced composite materials under axial shear," Int. J. Mech. Sci., 49, 1344-1354.

[20] Zou, M., Yu, B., Zhang, D., 2002, "An analytical solution for transverse thermal conductivities of unidirectional fibre composites with thermal barrier," J. Phys. D: Appl. Phys., 35, 1867-1874.

[21] Bisegna, P., Caselli, F., 2008, "A simple formula for the effective complex conductivity of periodic fibrous composites with interfacial impedance and applications to biological tissues," J. Phys. D: Appl. Phys., 41, 115506.

[22] Perrins, W. T., McKenzie, D. R., McPhedran, R. C., 1979, "Transport properties of regular arrays of cylinders," Proc. Royal Soc. London A, 369, 207-225.